Proceedings of the
47th IEEE Conference on Decision and Control
Cancun, Mexico, Dec. 9-11, 2008

Analysing the interaction between braking control and speed estimation: the case of two-wheeled vehicles

Mara Tanelli, Maria Prandini, Fabio Codecà, Alessandro Moia and Sergio M. Savaresi

Abstract— **The availability of actuators capable of a very fine-grained modulation of both traction and braking torques makes the design of slip-based braking control strategies for two-wheeled vehicles a real possibility. As the wheel slip cannot be directly measured, one has to use some estimate of the vehicle speed. The most commonly used speed estimate for two-wheeled vehicles is the fastest wheel speed. This paper investigates the interaction between control and estimation in braking control design for two-wheeled vehicles. Specifically, it is shown that a slip controller can be designed which guarantees global asymptotic stability under perfect knowledge of the vehicle speed. Conversely, when such a controller is fed by the fastest wheel speed stability is lost.**

I. Introduction

Nowadays, four-wheeled vehicles are equipped with many different active control systems which enhance driver's and passengers' comfort and safety. Among these active control systems, the Anti-lock Braking System (ABS) has recently become a standard equipment on all cars, see *e.g.,* [1], [2], [3], [4]. In the field of two-wheeled vehicles, instead, the development of electronic control systems is still in its infancy, and only few commercial motorbikes are equipped with ABS. The current trend in automotive braking control system design is to move from threshold-based discrete control logics, mainly relying on wheel deceleration measurements, to more standard continuous slip-control (see e.g., [2], [5], [1]). The main motivation behind this major change in ABS design is due to the new actuators (both electro-hydraulic and electro-mechanical) which are replacing hydraulic brakes with discrete dynamics and which enable a continuous modulation of the braking torque, thereby allowing to formulate slip-control as a classical regulation problem. This trend is also affecting the two-wheeled vehicles field, [6], and it is fostered by the introduction of actuators capable of a very fine-grained modulation of both traction and braking torque as, for instance, the electric motors used as propulsion and braking systems in the latest generation of electric scooters. However, since the wheel slip cannot be directly measured, the vehicle longitudinal speed must be estimated to perform slip regulation. While speed estimation is a well-studied problem in four-wheeled vehicles, see e.g., [7],[8], this is not the case for two-wheeled vehicles. Estimating a two-wheeled vehicle speed is a far more complex task due to its peculiar dynamics. The presence of a single axis, the high sensitivity to load variations and the strong coupling between the component rigid bodies due to chassis and suspensions geometry make it nearly impossible to seamlessly transfer the know-how gained in four-wheeled vehicle speed estimation to the two-wheeled vehicles context. As a matter of fact, the most commonly used speed estimation method for two-wheeled vehicles is as simple as setting the vehicle speed equal to the fastest wheel speed, which can be easily measured by wheel encoders. Thus, it is of particular interest to investigate the interactions between braking control and speed estimation. This paper analyzes this interaction with reference to the in-plane dynamics of a two-wheeled vehicle, assuming that the braking maneuver is carried out on a straight line. It is shown that, under perfect speed knowledge, a slip controller can be designed which guarantees the existence of a unique equilibrium that is globally asymptotically stable for all choices of the set point at the front and rear wheels and for all road conditions. Conversely, when such a controller is fed by the fastest wheel speed taken as estimate of the vehicle speed, stability is lost. The obtained results suggest that the slip controller and the speed estimation algorithm, which in the industrial practice are often responsibility of different teams, should be carefully designed through a coordinate effort.

This work has been partially supported by MIUR project "New methods for Identification and Adaptive Control for Industrial Systems". M. Tanelli, M. Prandini, S. M. Savaresi, F. Codecà and A. Moia are with Dipartimento di Elettronica e Informazione, Politecnico di Milano, Piazza L. da Vinci 32, 20133 Milano, Italy. e-mail:{tanelli,prandini,savaresi,codeca,moia}@elet.polimi.it M. Tanelli is also with the Dipartimento di Ingegneria dell'Informazione e Metodi Matematici, Università degli studi di Bergamo, Via Marconi 5, 24044, Dalmine (BG), Italy.

II. Two-wheeled vehicle model

Motivated by the fact that we consider braking maneuvers taking place on a straight line, we adopt a simplified in-plane model of a two-wheeled vehicle, where the dynamic load transfer is assumed to be proportional to the vehicle deceleration only. Namely, the two-wheeled vehicle dynamics are described by the following set of equations

$$\begin{cases} J\dot{\omega}_f = r_f F_{x_f} - T_{b_f} \\ J\dot{\omega}_r = r_r F_{x_r} - T_{b_r} \\ m\dot{v} = -F_{x_f} - F_{x_r}, \end{cases} \tag{1}$$

where ω_f and ω_r [rad/s] are the angular speed of the front and rear wheels, respectively, $v\,[m/s]$ is the longitudinal speed of the vehicle center of mass, T_{b_f} and T_{b_r} [Nm] are the front and rear braking torques, F_{x_f} and F_{x_r} [N] are the front and rear longitudinal tire-road contact forces, $J\,[kg\,m^2]$, $m\,[kg]$ and $r_f = r_r = r\,[m]$ are the moment of inertia of the wheel, the vehicle mass, and the wheel radius, respectively (see Figure 1). For simplicity, we assume that the front and rear wheel radiuses are equal and denote both with r. The system is nonlinear due to the dependence of F_{x_i}, $i = \{f,r\}$, on the state variables v and ω_i, $i = \{f,r\}$. The expression of F_{x_i} as a function of these variables is involved and influenced by

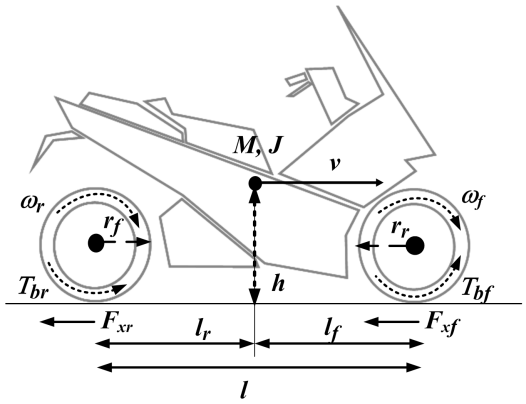

Fig. 1. In-plane model of a two-wheeled vehicle.

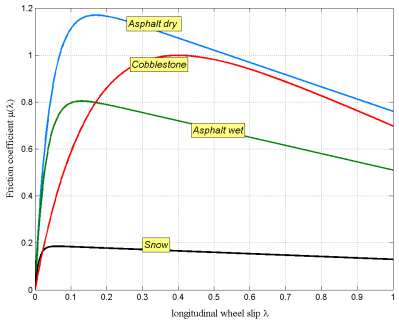

Fig. 2. Behavior of the function $\mu(\cdot;\vartheta)$ in different road conditions.

a large number of features of the road, tire, and suspension; however, it can be approximated as, [9]

$$F_{x_i} = F_{z_i}\,\mu(\lambda_i, \beta_{i_t}; \vartheta), \quad i = \{f, r\}, \tag{2}$$

where F_{z_i} is the vertical force at the tire-road contact point and $\mu(\cdot,\cdot;\vartheta)$ is a function of the longitudinal slip $\lambda_i \in [0,1]$, which, during braking, is defined as

$$\lambda_i = (v - \omega_i r)/v; \tag{3}$$

and of the wheel side-slip angle β_{i_t}. Vector ϑ in $\mu(\cdot,\cdot;\vartheta)$ represents the set of parameters that identify the tire-road friction condition. Since for braking maneuvers performed along a straight line one can set the wheel side-slip angle equal to zero ($\beta_{i_t} = 0$), we shall omit the dependence of F_{x_i} on β_{i_t} and denote the μ function as $\mu(\cdot;\vartheta)$.

Remark 2.1: It is worth mentioning that the results in this work remain valid if we remove the assumption that $\beta_{i_t} = 0$. In fact, changes in β_{i_t} cause a shift in the peak position of the $\mu(\cdot;\vartheta)$ curve and act as a scaling factor (in this resembling the effect of changes in the vertical load). Accordingly, as the controller is designed assuming no knowledge both of the current road conditions and of the value of the vertical load, it can handle non-zero values of β_{i_t}. ■

Many empirical analytical expressions for function $\mu(\cdot;\vartheta)$ have been proposed in the literature. A widely-used expression (see [9]) is

$$\mu(\lambda;\vartheta) = \vartheta_1(1 - e^{-\lambda\vartheta_2}) - \lambda\vartheta_3, \tag{4}$$

where ϑ_i, $i = 1,2,3$, are the three components of vector ϑ. By changing the values of these three parameters, many different tire-road friction conditions can be modeled. In Figure 2 the shape of $\mu(\cdot;\vartheta)$ in four different conditions is displayed.

From now on, for ease of notation, the dependency of μ on ϑ will be omitted, and the function in equation (4) will be referred to as $\mu(\lambda)$. To describe the load transfer phenomena between front and rear axles, we model the vertical force on the front and rear wheels as follows

$$\begin{aligned} F_{z_f} &= \frac{mgl_r}{l} - \frac{mh}{l}\dot{v} = W_f - \Delta_{F_z}\dot{v} \\ F_{z_r} &= \frac{mgl_f}{l} + \frac{mh}{l}\dot{v} = W_r + \Delta_{F_z}\dot{v}, \end{aligned} \tag{5}$$

where (see also Figure 1) l is the wheelbase, l_f and l_r are the distances between the projection of the center of mass on the road and the front and rear wheel contact points, respectively, h is the height of the center of mass and g is the gravitational acceleration. Note that $\dot{v}$ is the vehicle *acceleration*, hence negative during braking.

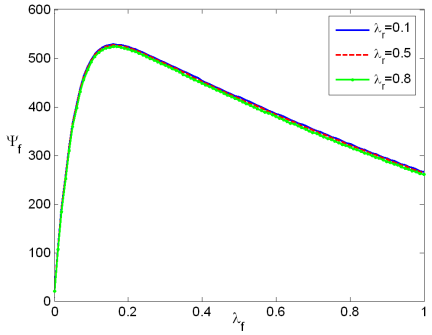

(a)

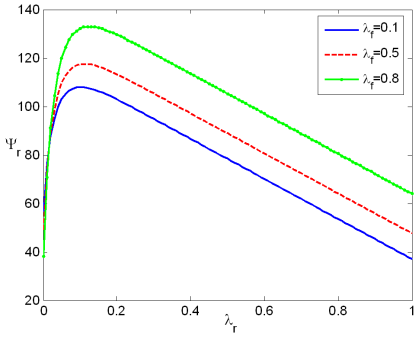

(b)

Fig. 3. Plot $\Psi_f(\cdot,\lambda_r)$ (a) for different values of λ_r: $\lambda_r = 0.1$ (solid line), $\lambda_r = 0.5$ (dashed line) and $\lambda_r = 0.1$ (dotted line) and of $\Psi_r(\lambda_f,\cdot)$ for different values of λ_f (b), $\lambda_f = 0.1$ (solid line), $\lambda_f = 0.5$ (dashed line) and $\lambda_f = 0.1$ (dotted line)(b).

In system (1) the state variables are v and ω_i. As λ_i, v and ω_i are linked by the algebraic equation (3), it is possible to replace ω_i with λ_i as state variable. As for the last equation in (1), it is easily shown that it can be rewritten as

$$\dot{v} = -\frac{W_f\mu(\lambda_f) + W_r\mu(\lambda_r)}{m - \Delta_{F_z}(\mu(\lambda_f) - \mu(\lambda_r))},$$

by using expression (2) for F_{x_i} and incorporating the vertical force description (5). The equation governing the evolution in time of λ_i is obtained by plugging into $\dot{\lambda}_i = -\frac{r}{v}\dot{\omega}_i + \frac{r\omega_i}{v^2}\dot{v}$ the expression $\omega_i = \frac{v}{r}(1-\lambda_i)$ and that for $\dot{\omega}_i$ taken from (1), with F_{x_i} also in this case given by (2) together with the vertical force description (5). This leads to the set of equations

$$\begin{cases} \dot{\lambda_f} = -\frac{r}{Jv}\left(\Psi_f(\lambda_f,\lambda_r) - T_{b_f}\right) \\ \dot{\lambda_r} = -\frac{r}{Jv}\left(\Psi_r(\lambda_f,\lambda_r) - T_{b_r}\right) \\ \dot{v} = -\frac{W_f\mu(\lambda_f)+W_r\mu(\lambda_r)}{m-\Delta_{F_z}(\mu(\lambda_f)-\mu(\lambda_r))}, \end{cases} \tag{6}$$

where we set

$$\Psi_f(\lambda_f,\lambda_r) = \left[r(W_f - \Delta_{F_z}\dot{v})\mu(\lambda_f) - \frac{J}{r}(1-\lambda_f)\dot{v}\right] \tag{7}$$

$$\Psi_r(\lambda_f,\lambda_r) = \left[r(W_r + \Delta_{F_z}\dot{v})\mu(\lambda_r) - \frac{J}{r}(1-\lambda_r)\dot{v}\right]. \tag{8}$$

Figures 3(a) and 3(b) show a plot of the functions $\Psi_f(\cdot,\lambda_r)$ and $\Psi_r(\lambda_f,\cdot)$, respectively, obtained for different values of λ_r and λ_f. As it is apparent by inspecting these figures, the front wheel behavior is substantially independent from that of the rear wheel, while the latter is strongly coupled to the front one. In the following, we shall disregard the dependence of $\Psi_f(\lambda_f,\lambda_r)$ from λ_r and adopt the notation $\Psi_f(\lambda_f)$.

III. Problem formulation and main results

In what follows it is assumed that the longitudinal dynamics of the vehicle (expressed by the state variable v) are significantly slower than the rotational dynamics of the wheels (expressed by the state variables λ_i or ω_i) due to the differences in inertia. Henceforth, v is considered as a slowly time-varying parameter when analyzing the evolution of λ_i (see *e.g.*, [2], [3]). Under this assumption, the third equation (center of mass dynamics) in (6) is neglected, and the model reduces to a second order model of the wheels dynamics only. Moreover, to concentrate on the core of the problem and to provide simple yet insightful results, for analysis purposes a simple proportional feedback controller is considered. Needless to say, the performance of proportional controllers can be improved by higher order control architectures, but the basic results and conclusions remain untouched, as shown in Section IV by simulation.

We first analyze the case where the vehicle speed v is known, so that an error-free measure of the controlled variables $\lambda_i, i = \{r,f\}$ is available. In this case, letting

$$T_{b_f} = k_f(\lambda_f^* - \lambda_f), \quad T_{b_r} = k_r(\lambda_r^* - \lambda_r), \tag{9}$$

where λ_f^* and λ_r^* are the set-point values for the front and rear wheel slip, respectively, and k_f, k_r are positive constants, the closed-loop dynamics become

$$\begin{aligned} \dot{\lambda_f} &= -\frac{r}{Jv}\left[\Psi_f(\lambda_f) - k_f(\lambda_f^* - \lambda_f)\right] \\ \dot{\lambda_r} &= -\frac{r}{Jv}\left[\Psi_r(\lambda_f,\lambda_r) - k_r(\lambda_r^* - \lambda_r)\right]. \end{aligned} \tag{10}$$

For the closed-loop system (10), we can state the following result.

Proposition 3.1: Consider the closed-loop system described by (10) with $v > 0$, and let $\lambda_i^* \in (0,1)$, $i = \{r,f\}$. Then, there exist positive gain values $\bar{k}_f$ and $\bar{k}_r$ such that, for any $k_f > \bar{k}_f$ and $k_r > \bar{k}_r$, the closed-loop system admits a unique globally asymptotically stable equilibrium for all initial conditions $\lambda_f(0), \lambda_r(0) \in (0,1)$, for all choices of λ_f^* and λ_r^* and for all road conditions.

Proof: Fix the set-point values $\lambda_f^*, \lambda_r^* \in (0,1)$. Let $(\tilde{\lambda}_f, \tilde{\lambda}_r)$ be an equilibrium of system (10) associated with λ_f^*, λ_r^*, i.e.,

$$\begin{cases} \Psi_f(\tilde{\lambda}_f) = k_f(\lambda_f^* - \tilde{\lambda}_f) \\ \Psi_r(\tilde{\lambda}_f, \tilde{\lambda}_r) = k_r(\lambda_r^* - \tilde{\lambda}_r). \end{cases} \tag{11}$$

As a preliminary step, we rewrite the equations (10) in a form that is more useful for analyzing the stability properties of $(\tilde{\lambda}_f, \tilde{\lambda}_r)$. We start from the equation governing λ_r

$$\begin{aligned} \dot{\lambda_r} &= -\frac{r}{Jv}\Big\{k_r(\lambda_r - \tilde{\lambda}_r) + \Psi_r(\tilde{\lambda}_f,\lambda_r) - k_r(\lambda_r^* - \tilde{\lambda}_r) \\ &\quad + \Psi_r(\lambda_f,\lambda_r) - \Psi_r(\tilde{\lambda}_f,\lambda_r)\Big\} \\ &= -\frac{r}{Jv}\Big\{(\lambda_r - \tilde{\lambda}_r)\Big[k_r + \frac{\Psi_r(\tilde{\lambda}_f,\lambda_r) - \Psi_r(\tilde{\lambda}_f,\tilde{\lambda}_r)}{\lambda_r - \tilde{\lambda}_r}\Big] \\ &\quad + \Psi_r(\lambda_f,\lambda_r) - \Psi_r(\tilde{\lambda}_f,\lambda_r)\Big\}, \end{aligned}$$

where the first equality is obtained by adding and subtracting $k_r\tilde{\lambda}_r$ and $\Psi_r(\tilde{\lambda}_f,\lambda_r)$ to the expression within the brackets in (10), whereas the second equality is obtained using the equilibrium condition (11).

A similar procedure applied to the equation in (10) governing λ_f leads to the following equivalent form for the closed-loop system equations (10)

$$\begin{aligned} \dot{\lambda_f} &= -\frac{r}{Jv}\Big[k_f + \alpha_f(\lambda_f)\Big](\lambda_f - \tilde{\lambda}_f) \\ \dot{\lambda_r} &= -\frac{r}{Jv}\Big[k_r + \alpha_r(\lambda_r)\Big](\lambda_r - \tilde{\lambda}_r) + \gamma(\lambda_f,\lambda_r), \end{aligned} \tag{12}$$

where we set

$$\alpha_f(\lambda_f) = \frac{\Psi_f(\lambda_f) - \Psi_f(\tilde{\lambda}_f)}{\lambda_f - \tilde{\lambda}_f}, \; \alpha_r(\lambda_r) = \frac{\Psi_r(\tilde{\lambda}_f,\lambda_r) - \Psi_r(\tilde{\lambda}_f,\tilde{\lambda}_r)}{\lambda_r - \tilde{\lambda}_r},$$

$$\gamma(\lambda_f,\lambda_r) = -\frac{r}{Jv}[\Psi_r(\lambda_f,\lambda_r) - \Psi_r(\tilde{\lambda}_f,\lambda_r)].$$

Note that we are studying a cascade system where λ_f evolves independently of λ_r and affects the dynamics of λ_r through the additive term $\gamma(\lambda_f,\lambda_r)$, which vanishes when λ_f is at the equilibrium, i.e., $\gamma(\tilde{\lambda}_f,\lambda_r) = 0$, $\forall\lambda_r$. Also, $\alpha_f(\lambda_f)$ represents the slope of the straight line intersecting the curve $\Psi_f(\cdot)$ in the two points of coordinates λ_f and $\tilde{\lambda}_f$. Thus, $\alpha_f(\lambda_f)$ is lower bounded by the negative steepest slope of the friction curve $\Psi_f(\cdot)$ obtained in different road conditions ϑ. A similar geometric interpretation holds for $\alpha_r(\lambda_r)$.

We next show that, for $i \in \{f,r\}$, if k_i is large enough, then the equilibrium $\tilde{\lambda}_i$ of the subsystem

$$\dot{\lambda}_i = -\frac{r}{Jv}\Big[k_i + \alpha_i(\lambda_i)\Big](\lambda_i - \tilde{\lambda}_i) \tag{13}$$

is globally exponentially stable (GES) and, hence, also globally asymptotically stable (GAS). Note that subsystem (13) with $i = r$ is obtained from the cascade system (12) by removing the interconnection term $\gamma(\lambda_f, \lambda_r)$ and setting λ_f at the equilibrium. Consider the candidate Lyapunov function $V(\lambda_i) = (\lambda_i - \tilde{\lambda}_i)^2/2$, which, by construction, is positive definite ($V(\lambda_i) > 0$ for all $\lambda_i \neq \tilde{\lambda}_i$, and $V(\tilde{\lambda}_i) = 0$) and radially unbounded. The time derivative of V along the subsystem trajectories is

$$\dot{V}(\lambda_i) = (\lambda_i - \tilde{\lambda}_i)\dot{\lambda}_i = -\frac{r}{Jv}\Big[k_i + \alpha_i(\lambda_i)\Big](\lambda_i - \tilde{\lambda}_i)^2.$$

Thus, recalling the definition of $\alpha_f(\lambda_f)$ and $\alpha_r(\lambda_r)$, if

$$k_f > \bar{k}_f = -\min_{\vartheta, \lambda_f, \lambda_f'} \frac{\Psi_f(\lambda_f) - \Psi_f(\lambda_f')}{\lambda_f - \lambda_f'} \tag{14}$$

$$k_r > \bar{k}_r = -\min_{\vartheta, \lambda_r, \lambda_r', \lambda_f'} \frac{\Psi_r(\lambda_f', \lambda_r) - \Psi_r(\lambda_f', \lambda_r')}{\lambda_r - \lambda_r'} \tag{15}$$

we get that $\dot{V}(\lambda_i) < -c_i(\lambda_i - \tilde{\lambda}_i)^2$, with $c_i > 0$, which concludes the proof that the equilibrium $\tilde{\lambda}_i$ of subsystem (13) is GES, [10]. To complete the proof, we need to show that the cascade interconnection of the two subsystems through $\gamma(\lambda_f, \lambda_r)$ does not destroy global asymptotic stability. To prove that the cascade of the two subsystems is GAS, [11], [12], it is enough to show that the λ_r dynamics have the Converging-Input-Bounded-State (CIBS) property with respect to the input λ_f, which is guaranteed if the trajectories of the full system (10) exist for all $t \geq 0$ and are bounded. The GES property of the equilibrium $\tilde{\lambda}_f$ guarantees that we are dealing with a converging input, *i.e.*, $\lambda_f(t) \to \tilde{\lambda}_f$ as $t \to \infty$. From the expression of $\Psi_r(\lambda_f, \lambda_r)$ (8) (see also Figure 3(b)), one may notice that the closed-loop λ_r dynamics in (10) with $k_r > \bar{k}_r$ – which can be compactly written in the form $\dot{\lambda}_r = g(\lambda_f, \lambda_r)$ – are such that $g(\cdot,\cdot)$ is C^1 in $H = [0,1] \times [0,1]$ and bounded for all $\lambda_f, \lambda_r \in (0,1)$. This implies that $g(\cdot,\cdot)$ is Lipschitz in both arguments on H. Note also that H is compact; moreover, analyzing the vector fields of (10) at the boundary of H, one finds that H is positively invariant. This, together with compactness and Lipschitz continuity, [10], ensures that a unique solution exists for all $t \geq 0$ and that it is bounded. Hence the thesis follows. ■

Remark 3.1: A solution to (11) always exists for $k_f, k_r > 0$ and can be graphically identified by first intersecting $\Psi_f(\lambda_f)$ in Figure 3(a) with the line of negative slope $-k_f$ cutting the λ_f axis in λ_f^* to determine $\tilde{\lambda}_f$, and then intersecting $\Psi_r(\tilde{\lambda}_f, \lambda_r)$ in Figure 3(b) with the line of negative slope $-k_r$ cutting the λ_r axis in λ_r^* to determine $\tilde{\lambda}_r$. If k_f and k_r satisfy the bound for the global asymptotic stability result to hold, the equilibrium is unique. Note also that, as we are using a proportional controller, the values $\tilde{\lambda}_f$ and $\tilde{\lambda}_r$ are in general different from λ_f^* and λ_r^*. From (11), however, it is clear that $\tilde{\lambda}_f$ and $\tilde{\lambda}_r$ are close to λ_f^* and λ_r^* if the gains k_r and k_f are sufficiently large. ■

Remark 3.2: In [3], a similar condition on the gain of a proportional slip controller (gain greater than the steepest negative slope of the friction curve for all road conditions) for *local* stability was derived based on the linearized quarter-car model. Proposition 3.1 thus extends the results in [3] to the in-plane model (10), and also from a local to a global stability result. ■

Proposition 3.1 shows that, if v is perfectly known, the system dynamics (10) can be stabilized by a proportional controller, provided that the controller gains are properly chosen. Now, we consider the case in which the vehicle speed v cannot be directly measured, but it is estimated as the fastest wheel speed. Even though this estimation may appear quite rough, it is in fact the common practice in the two wheeled-vehicles context, where it appears to be very difficult to set-up an efficient speed estimation algorithm, [6]. Formally, the vehicle speed is estimated as $\hat{v} = \max\{\omega_f, \omega_r\} r$. Correspondingly, given the definition (3) of the wheel slip, the estimate of the front wheel slip $\hat{\lambda}_f$ is given by

$$\begin{aligned} \hat{\lambda}_f &= 1 - \frac{\omega_f}{\omega_f} = 0, && \text{if } \omega_f \geq \omega_r \Leftrightarrow \lambda_f \leq \lambda_r, \\ \hat{\lambda}_f &= 1 - \frac{\omega_f}{\omega_r} = \frac{\lambda_f - \lambda_r}{1 - \lambda_r}, && \text{if } \omega_f < \omega_r \Leftrightarrow \lambda_f > \lambda_r. \end{aligned} \tag{16}$$

Analogous expressions hold for the rear slip estimate $\hat{\lambda}_r$. Thus, if the proportional controller (9) is used with λ_i replaced by $\hat{\lambda}_i$ $i = \{f, r\}$, the closed-loop system dynamics keep continuous but have two different expressions in two different regions of the state space

Region I ($\lambda_f \leq \lambda_r$)**:**

$$\begin{aligned} \dot{\lambda_f} &= -\frac{r}{Jv}\left(\Psi_f(\lambda_f) - k_f \lambda_f^*\right) \\ \dot{\lambda_r} &= -\frac{r}{Jv}\left(\Psi_r(\lambda_f, \lambda_r) - k_r\left[\lambda_r^* - \frac{\lambda_r - \lambda_f}{1 - \lambda_f}\right]\right), \end{aligned} \tag{17}$$

Region II ($\lambda_f > \lambda_r$)**:**

$$\begin{aligned} \dot{\lambda_f} &= -\frac{r}{Jv}\left(\Psi_f(\lambda_f) - k_f\left[\lambda_f^* - \frac{\lambda_f - \lambda_r}{1 - \lambda_r}\right]\right) \\ \dot{\lambda_r} &= -\frac{r}{Jv}\left(\Psi_r(\lambda_f, \lambda_r) - k_r \lambda_r^*\right). \end{aligned} \tag{18}$$

In Proposition 3.2, we analyze the behavior of the system described by (17) and (18), when the gains of the wheel slip controller are chosen to be high, as suggested by Proposition 3.1 and the considerations in Remark 3.1.

Proposition 3.2: Consider the closed-loop system described by equations (17)-(18) with $k_f > \max_{\lambda_f} \Psi_f(\lambda_f)$ and $k_r > \max_{\lambda_f, \lambda_r} \Psi_r(\lambda_f, \lambda_r)$. Then, there exist set-point values $\lambda_i^* \in (0,1), i = \{r, f\}$ such that, for all initial conditions $\lambda_f(0)$, $\lambda_r(0) \in (0,1)$ the wheels lock, that is $\lambda_i \to 1, i = \{r, f\}$.

Proof: Given the bounds on the controller gains, we can choose $\lambda_i^* \in (0,1), i = \{r, f\}$ so as to satisfy

$$\begin{aligned} &\Psi_f(\lambda_f) - k_f \lambda_f^* < 0, \forall \lambda_f \\ &\Psi_r(\lambda_f, \lambda_r) - k_r \lambda_r^* < 0, \forall \lambda_f, \lambda_r. \end{aligned} \tag{19}$$

Three different situations may occur: i) the state of the system remains in Region I from some time $\bar{t} \geq 0$ on: $\lambda_f(t) \leq \lambda_r(t)$, $t \geq \bar{t}$; ii) the state of the system remains in Region II from some time $\bar{t} \geq 0$ on: $\lambda_f(t) > \lambda_r(t)$, $t \geq \bar{t}$; iii)

the state of the system keeps switching between Region I and Region II. Let us start considering case i). By the first equation in (17) and (19), within Region I, we have both $\dot{\lambda}_f > 0$ and $\lambda_r > \lambda_f$. Thus, as time grows, $\lambda_f \to 1$, so that the front wheel locks and, as $\lambda_r > \lambda_f$, also $\lambda_r \to 1$. The same reasoning applies to case ii). As for case iii), we shall prove by contradiction that it cannot actually occur. To this purpose, we start by observing that the time derivative of $\Delta\lambda = \lambda_f - \lambda_r$ for $\lambda_f = \lambda_r = \lambda$ is given by

$$\Delta\dot{\lambda} = -\frac{r}{Jv}\Big(r(W_f - W_r - 2\Delta_{F_z}\dot{v})\mu(\lambda) - k_f\lambda_f^* + k_r\lambda_r^*\Big), \quad (20)$$

which is obtained based on (17) and the definitions of $\Psi_f(\cdot)$ and $\Psi_r(\cdot,\cdot)$ in equations (7) and (8). Thus, on the boundary between Region I and Region II, $\Delta\dot{\lambda}$ is zero for those values of $\lambda_f = \lambda_r = \lambda$ satisfying the equation

$$\mu(\lambda) = [k_f\lambda_f^* - k_r\lambda_r^*]/[r(W_f - W_r - 2\Delta_{F_z}\dot{v})].$$

Recalling the expression for $\mu(\cdot)$ in (4), we then have that there is a single value, say $\overline{\lambda}$, such that $\Delta\dot{\lambda}(t) = 0$ when $\lambda_f(t) = \lambda_r(t) = \overline{\lambda}$. Assume now by contradiction that there exists $\{t_k\}_{k\geq 0}$, with $t_{k+1} > t_k \geq 0$, $k \geq 0$, such that $\lambda_f(t) > \lambda_r(t)$, $t \in (t_{2h}, t_{2h+1})$, and $\lambda_f(t) \leq \lambda_r(t)$, $t \in (t_{2h+1}, t_{2h+2})$, $h \geq 0$. Set $\lambda_k := \lambda_f(t_k) = \lambda_r(t_k)$. We next show that from this assumption it follows that

$$\lambda_{k+1} > \lambda_k, k \geq 0. \quad (21)$$

Note that (21) implies that there exists a sequence $\{\lambda_k\}$ of increasing values of λ such that $\Delta\dot{\lambda}$ in (20) keeps changing sign. Because of the continuity of $\Delta\dot{\lambda}$ as a function of λ, this contradicts the fact that $\Delta\dot{\lambda} = 0$ on a single point ($\lambda_f = \lambda_r = \overline{\lambda}$) of the boundary between Region I and Region II, thus concluding the proof of the proposition. For the state to commute at time t_{2h} from Region I where $\lambda_f - \lambda_r \leq 0$ to Region II where $\lambda_f - \lambda_r > 0$, it should hold that $\lambda_f(t_{2h}) = \lambda_r(t_{2h}) = \lambda_{2h}$ and $\Delta\dot{\lambda}(t_{2h}) > 0$. By a similar reasoning, it is easily seen that for the state to commute at time $t_{2h+1} > t_{2h}$ back from Region II to Region I, $\lambda_f(t_{2h+1}) = \lambda_r(t_{2h+1}) = \lambda_{2h+1}$ and $\Delta\dot{\lambda}(t_{2h+1}) \leq 0$. Thus, $\lambda_{2h+1} \neq \lambda_{2h}$ because of the different sign of $\Delta\dot{\lambda}$ on the boundary at $\lambda_f = \lambda_r = \lambda_{2h}$ and $\lambda_f = \lambda_r = \lambda_{2h+1}$. Moreover, we know that $\lambda_{2h+1} \geq \lambda_{2h}$, since we have $\dot{\lambda}_f > 0$ within Region I, $\dot{\lambda}_r > 0$ within Region II, and both $\dot{\lambda}_f > 0$ and $\dot{\lambda}_r > 0$ on the boundary between Region I and Region II (this is a consequence of (19) and of the continuity of the vector field (17)-(18)). From $\lambda_{2h+1} \geq \lambda_{2h}$ and $\lambda_{2h+1} \neq \lambda_{2h}$, it follows that $\lambda_{2h+1} > \lambda_{2h}$. In a perfectly analogous way it can be shown that $\lambda_{2h+2} > \lambda_{2h+1}$, so that (21) is finally proven. ■

Remark 3.3: The result in Proposition 3.2 have been proved considering large values for the gains of the controller as suggested by a design of the controller that does not take into account the issue of speed estimation. As a matter of fact, considering the common set-point values for the application at hand, that is $\lambda^* \in [0.1, 0.25]$, one finds that the equilibrium (11) corresponding to lower gains $k_f < \max_{\lambda_f} \Psi_f(\lambda_f)$ and $k_r < \max_{\lambda_f,\lambda_r} \Psi_r(\lambda_f,\lambda_r)$, would take extremely low values, unappropriate for safely managing a braking maneuver. Thus, the only situation of potentially practical interest is that investigated in Proposition 3.2. ■

IV. Simulation Results and Performance Analysis

In Section III, we have considered a proportional controller of the front and rear wheel slips and shown that its performance dramatically deteriorates when the fastest wheel speed is used in place of the actual, not directly measurable, vehicle speed. We now present a simulation study which confirms that the results in Section III still hold when a PID controller is used instead of a simple proportional controller. Furthermore, we discuss what is the gain in performance potentially offered by a combined front and rear wheel slip control with respect to the front-braking-only solution that is currently adopted in most commercial two-wheeled vehicles. The simulation results presented in this section have been obtained with a detailed dynamical model of a two-wheeled vehicle, in which the suspensions dynamics are explicitly modeled, and tire elasticity and tire relaxation dynamics [9] are also taken into account. As for the actuator, a first order low-pass filter with 10Hz of bandwidth complemented with a pure delay of 10ms has been employed. The wheel slip controller has been implemented with a PID architecture. Both the front and rear wheel slip set-points have been set equal to $\lambda_f^* = \lambda_r^* = 0.22$.

Figure 4 shows a braking maneuver carried out with combined front and rear wheel slip control assuming perfect knowledge of the vehicle speed, i.e., the case discussed in Proposition 3.1. As can be seen Figure 4, when both the front and rear wheel slips λ_f and λ_r are regulated to the same set-point value, their estimated counterparts $\hat{\lambda}_f$ and $\hat{\lambda}_r$ obtained via (16) are zero at steady-state, as $\omega_f = \omega_r$. Not surprisingly, when the estimated front and rear wheel slips are used, i.e., the case discussed in Proposition 3.2, both wheels lock as shown in Figure 5.

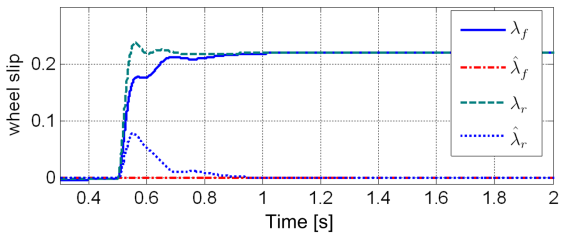

Fig. 4. Braking maneuver with front and rear wheel slip control based on measured vehicle speed. Actual front wheel slip (solid line), estimated front wheel slip (dash-dotted line), actual rear wheel slip (dashed line), estimated rear wheel slip (dotted line).

If the vehicle speed cannot be estimated with sufficient precision, a viable alternative in two-wheeled vehicle is that of braking with the front wheel only [6], [13], [14]. As a matter of fact, this is the current braking strategy on most commercial two-wheeled vehicles. Braking with both front and rear wheels has only recently become possible thanks to the new generation of actuators. If only front braking is used, then the rear wheel speed provides a good estimate of the vehicle speed given that the rear wheel rolls freely. The braking performance obtained with front braking only can be appreciated inspecting Figure 6, where front and rear wheel

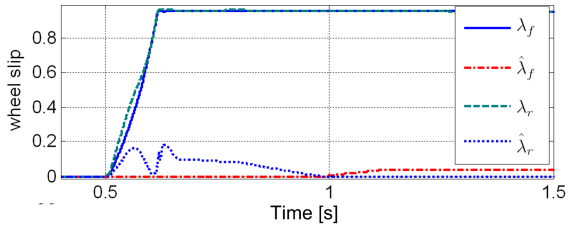

Fig. 5. Braking maneuver with front and rear wheel slip control based on estimated vehicle speed. Actual front wheel slip (solid line), estimated front wheel slip (dash-dotted line), actual rear wheel slip (dashed line), estimated rear wheel slip (dotted line).

slip λ_f and λ_r and their estimated counterparts $\hat{\lambda}_f$ and $\hat{\lambda}_r$ obtained via (16) are shown.

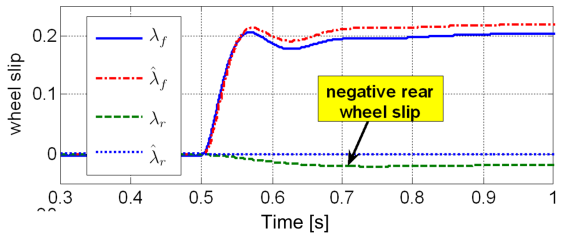

Fig. 6. Braking maneuver with front braking only. Actual front wheel slip (solid line), estimated front wheel slip (dash-dotted line), actual rear wheel slip (dashed line), estimated rear wheel slip (dotted line).

Note that the rear wheel slip in Figure 6 is *negative* and not equal to zero. Namely, the rear wheel provides a *traction* torque. This fact can be surprising at a first glance, but can be explained by observing that the rear wheel has a kinetic energy given by $\frac{1}{2}J\bar{\omega}_r^2$, where $\bar{\omega}_r$ is the rear wheel rotational speed at the beginning of the braking maneuver, and J is the inertia of the rear wheel. If the engine is disengaged during braking and only the front brake is used, this energy is not dissipated but it is transformed into a traction torque. This phenomenon clearly induces an increase in the braking distance when only the front brake is used. Nonetheless, as the rear wheel speed can be easily measured, if we impose to the rear wheel a braking torque equal to $T_{br} = -J\dot{\omega}_r$, the acceleration effect can be counteracted and the braking distance (in the case of front brake only) reduced. The results of front wheel braking with the compensation for the kinetic energy at the rear wheel are reported in Figure 7. As can be seen, now the rear wheel slip is forced to be equal to zero. This allows to significantly reduce the stopping distance.

Algorithm	X_{br} [m]	Performance loss [%]
Full slip control, v known	33.34 m	baseline
Full slip control, v estimated	wheel locking	n.a.
Front brake only, v estimated no rear traction compensation	51.32 m	54%
Front brake only, v estimated rear traction compensation	46.4 m	39.2%

TABLE I
PERFORMANCE OF THE BRAKING CONTROL STRATEGIES.

For comparison purposes, Table IV reports the stopping distance X_{br}[m] (from 100 to 0 km/h) obtained with the

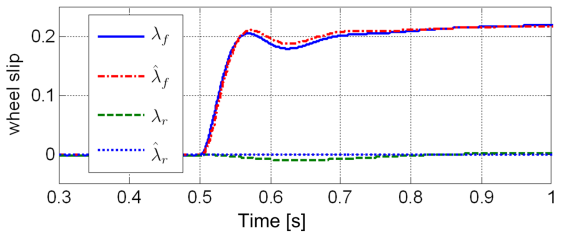

Fig. 7. Braking maneuver with front braking only and compensation of the positive rear wheel slip. Actual front wheel slip (solid line), estimated front wheel slip (dash-dotted line), actual rear wheel slip (dashed line), estimated rear wheel slip (dotted line).

considered algorithms, together with the percentage performance loss with respect to the best solution offered by combined front and rear slip control with perfect vehicle speed measurements. As can be seen, a significant performance loss occurs if one downgrades the braking control strategy to front-brake only. This loss of performance can be partially recovered by compensating the kinetic energy at the rear wheel. Notably, with the compensation, the performance loss is reduced from 54% to 39.2%. Nonetheless, if speed estimation cannot be achieved with sufficient precision, this downgrade might be necessary for the sake of safety.

REFERENCES

[1] S. Drakunov, U. Ozguner, P. Dix, and B. Ashrafi, "ABS control using optimum search via sliding modes," *IEEE Transactions on Control Systems Technology*, vol. 3, no. 1, pp. 79–85, 1995.
[2] T. Johansen, I. Petersen, J. Kalkkuhl, and J. Lüdemann, "Gain-scheduled wheel slip control in automotive brake systems," *IEEE Transactions on Control Systems Technology*, vol. 11, no. 6, pp. 799–811, November 2003.
[3] S. Savaresi, M. Tanelli, and C. Cantoni, "Mixed Slip-Deceleration Control in Automotive Braking Systems," *ASME Journal of Dynamic Systems, Measurement and Control*, vol. 129, no. 1, pp. 20–31, 2006.
[4] M. Tanelli, A. Astolfi, and S. Savaresi, "Robust nonlinear output feedback control for brake-by-wire control systems." *Automatica*, vol. 44, no. 4, pp. 1078–1087, 2008.
[5] K. Buckholtz, "Reference input wheel slip tracking using sliding mode control," in *SAE Technical Paper 2002-01-0301*, 2002.
[6] M. Corno, S. Savaresi, M. Tanelli, and L. Fabbri, "On optimal motorcycle braking." *Control Engineering Practice*, vol. 16, no. 6, pp. 644–657, 2008.
[7] L. Ray, "Nonlinear state and tire force estimation for advanced vehicle control," *IEEE Transactions on Control Systems Technology*, vol. 3, no. 1, pp. 117–124, 1995.
[8] M. Tanelli, S. Savaresi, and C. Cantoni, "Longitudinal Vehicle Speed Estimation for Traction and Braking Control Systems," in *Proceedings of the 2006 Conference on Control and Applications - CCA 2006, Munich, Germany*, 2006.
[9] U. Kiencke and L. Nielsen, *Automotive Control Systems*. Springer-Verlag, Berlin, 2000.
[10] H. Khalil, *Nonlinear Systems*. Upper Saddle River, New Jersey: 2nd Edition, Prentice Hall, 1996.
[11] E. Sontag, "Remarks on stabilization and input to state stability." in *Proceedings of the IEEE Conference on Decision and Control, Tampa, USA*, 1989, pp. 1376–1378.
[12] H. J. Sussmann and P. Kokotovic, "The peaking phenomenon and the global stabilization of nonlinear systems," *IEEE Transactions on Automatic Control*, vol. 36, no. 4, pp. 424–440, 1991.
[13] V. Cossalter, *Motorcycle Dynamics*. Milwaukee, USA: Race Dynamics, 2002.
[14] D. J. N. Limebeer, R. S. Sharp, and S. Evangelou, "The stability of motorcycles under acceleration and braking," *Proc. I. Mech. E., Part C, Journal of Mechanical Engineering Science*, vol. 215, pp. 1095–1109, 2001.